Civil Engineering Infrastructures Journal 2024, 57(1): 157-173
DOI: 10.22059/CEIJ.2023.353013.1899

RESEARCH PAPER

Pushover Analysis of Reinforced Concrete Moment-Resisting Frames to Account for the Variations of Axial Forces on the Moment Curvature Properties

Samadi, N.[1], Aghayari, R.[2] and Izadpanah, M.[3*]

[1] M.Sc., Department of Civil Engineering, Razi University, Kermanshah, Iran.
[2] Associate Professor, Department of Civil Engineering, Razi University, Kermanshah, Iran.
[3] Assistant Professor, Department of Civil Engineering, Kermanshah University of Technology, Kermanshah, Iran.

Received: 26 Dec. 2022; Revised: 09 May 2023; Accepted: 10 May 2023

ABSTRACT: Nonlinear static (pushover) analysis is widely used for analyzing structures, especially in the performance-based design method. Increasing the lateral load in pushover analysis causes changing the axial forces of beam-column members during the analysis. Whereas the axial load of beam-column elements can significantly affect the moment-curvature properties of these elements, in most pushover analyses, the moment-curvature curve of these elements is generally achieved based on the gravity axial loads and remain constant throughout the analysis. Furthermore, the confining action depends on the axial load of beam-column elements. In this study, a novel pushover analysis is developed to update the moment-curvature properties of beam-column elements based on the axial forces of these elements throughout the analysis. The confining effect is considered on the moment-curvature properties of beam-column elements as well. Furthermore, the influence of updating the moment-curvature properties is shown by comparing the responses of the updated and traditional pushover analyses. The method is applied to three reinforced concrete frames from the previous studies to assess the influence of the variation of moment-curvature properties on the capacity curve of these frames. Outcomes show that the variation of axial loads significantly affects the moment-curvature of beam-column elements especially for edge columns located in the lower stories of frames. Furthermore, considering the progressive changes of moment-curvature properties of beam-column elements during the pushover analysis accounting for the variations of axial forces leads to reducing the lateral load-carrying capacity e.g, ductility, secant stiffness ultimate strength, etc.

Keywords: Axial Force, Beam-Column, Confining Action, Moment-Curvature, Nonlinear Static Analysis.

1. Introduction

The nonlinear dynamic analysis is known as a robust method for predicting the seismic responses of structures. Inherent complexity and uncertainties are some

* Corresponding author E-mail: m.izadpanah@kut.ac.ir

difficulties that make civil engineers do not interest in using this method in practice. The nonlinear static analysis method is found as a substitute approach for nonlinear dynamic analysis due to less computational endeavors coupled with providing helpful information dealing with the lateral load capacity, potential failure mechanisms, and the sequence formation of plastic hinges of building structures. In pushover analysis, lateral load distribution is monotonically imposed on the structure until a predefined target displacement at the control node (usually considered the roof displacement) is reached. The axial load of beam-column elements depends on the imposed lateral load and varies during the pushover analysis. On the whole, the moment-curvature characteristics of each beam-column element are calculated at the first step of analysis considering simply the gravity axial loads and remaining constant throughout the analysis while neglecting the influence of the variation of its axial load.

Studies of Gulkan and Sozen (1974) and Fajfar and Fischinger (1988) are known as the first investigations of pushover analysis. More complete pushover analyses have been introduced in various code provisions e.g., FEMA273, ATC-40, and Eurocode 8. Pushover analysis has some limitations and shortcomings that have motivated researchers to develop some boost pushover methods to mitigate these deficiencies. In the conventional pushover procedure, a constant lateral load distribution is used along the height of the building and increased until the target displacement reaches. This constant lateral load pattern raised the question that how much this force distribution can reflect the inertial loads imposed on the structures subjected to seismic excitations. Hence, numerous studies have focused on obtaining an appropriate lateral load pattern to improve the responses of pushover analysis (e.g., Chopra and Goel, 2002; Antoniou and Pinho, 2004; Rahmani et al., 2018; Amini and Poursha, 2018; Habibi et al., 2019; Bakalis and Makarios, 2021; Worku and Hsiao, 2022; Lherminier et al., 2023). Evaluation of the responses of pushover analysis has been addressed in many studies (Fajfar and Gašperšič, 1996; Gupta and Krawinkler; 2000; Mwafy and Elnashai, 2001; Olivito and Porzio, 2019; Hassan and Reyes, 2020; Cao et al., 2021). Regarding the works of Fajfar and Gašperšič (1996) and Gupta and Krawinkler (2000), it was found that distributing lateral loads along the height of buildings proportional to the main vibration mode leads to an appropriate estimation of the seismic responses in low-rise buildings. However, some studies e.g., Krawinkler and Seneviratna (1998) and Mwafy and Elnashai (2001) evaluated the validity of the lateral load pattern proportional to the first mode for high-rise or irregular structures. They concluded that pushover analysis does not present reasonable responses for these categories of buildings since the influence of higher modes on the responses is significant.

As per the previous investigations, the conventional pushover analysis cannot reflect the higher mode effects and the progressive variations of the dynamic characteristics (Lawson et al., 1994; Elnashai, 2001; Antoniou and Pinho, 2004). A multi-run method with an invariant lateral load distribution matching each desired mode was developed by Chopra and Goel (2002). In this method, the achieved responses were combined applying a combination way such as SRSS or CQC. Chopra and Goel (2004) improved the previous method and used it for predicting asymmetric-plan buildings' responses. Kalkan and Kunnath (2006) put forward a novel pushover analysis method using adaptive multimodal displacement distribution for estimating the seismic response of structures. The proposed method was used for two existing steel moment frames. They demonstrated that the procedure gives reasonable results in comparison with nonlinear dynamic analysis.

Reyes and Chopra (2011) extended the model pushover analysis for predicting the

seismic responses of buildings simultaneously under two horizontal components of an earthquake. This procedure (named practical modal pushover analysis) was applied to calculating the seismic responses of two tall buildings (48- and 62-story) and the outcomes were compared with those of modal pushover analysis and nonlinear response history analysis. Habibi (2011) conducted a nonlinear sensitivity analysis of reinforced concrete frames taking both axial and flexural effects into account. He derived sensitivity equations on the base of the pushover procedure as a powerful tool for the nonlinear analysis of buildings in performance base design.

The observations of Nazri and Alexander (2014) showed that lateral load distribution should be decreased instead of increasing along the height of the structure. Nazri and Alexander (2015) demonstrated that the inverse parabolic lateral load pattern presents a proper prediction of the capacity of structures. Rahmani et al. (2018) developed a new nonlinear static analysis to evaluate the seismic performance of tall buildings. This model was capable of considering the higher modes effects coupled with the progressive changes in structural characteristics during the nonlinear response. Comparing the responses of different types of pushover analyses with nonlinear time history analysis showed that the proposed procedure presented more reasonable outcomes than other pushover methods (e.g., upper-bound pushover, improved upper-bound, modal pushover analysis, displacement-based adaptive pushover methods).

A multi-mode adaptive displacement-based pushover procedure for predicting the seismic responses of Reinforced Concrete (RC) moment-resisting frames was developed by Jalilkhani et al. (2020). In this procedure, the seismic responses of structures were predicted utilizing several multi-stage modal pushover analyses. The seismic structural demands of four RC moment resisting frames with various stories were calculated using the developed method, the modal pushover, as well as consecutive modal pushover methods. Results verified the efficiency of the proposed method in comparison with nonlinear dynamic analysis (considered as a benchmark).

Daei and Poursha (2021) evaluated the performance of different pushover methods. The structural demands of three RC frames subjected to pulse-like and non-pulse-like ground motions were achieved using various pushover analyses. Results showed that some procedures present reasonable responses for pulse-like excitations, some for non-pulse-like ground motions, and some for both of them. A multi-direction pushover method was developed for the evaluation of the seismic performance of RC buildings with torsional irregularity by Ghayoumian and Emami (2020). Pushover analysis was used in a plethora of studies (e.g., Costa et al., 2017; Ozgenoglu and Arıcı, 2017; Tian and Qiu, 2018; Izadpanah and Habibi, 2018a; Moradi and Tavakoli, 2020; Kheirollahi et al., 2021; Dehghani and Soltani Mohajer, 2022; Wang et al., 2023; Zhou et al., 2023; etc.).

Lu and Li (2023) studied the efficacy of the energy-based modal pushover analysis and the direct vectorial addition based pushover method in estimating the curvature ductility demands of tall single-column piers. They compared the responses of the piers acquired from pushover analyses with those calculated using incremental dynamic analysis. It was found that the curvature ductility demands can be predicted effectively using the direct vectorial addition based pushover method.

Faruk et al. (2023) conducted a comparative study on the performance of buckling restrained bracing and fluid viscous damper (as two types of energy dissipators) used in reinforced concrete buildings. Taking advantages of pushover analysis, the responses of four buildings equipped by these dissipators were acquired and compared. Lawson et al. (1994) and

Krawinkler and Seneviratna (1998) evaluated the advantages and deficiencies of pushover analysis.

The literature proves that despite of the plethora research for improving pushover analysis, the progressive changes of the moment-curvature characteristics of beam-column elements due to the variation of their axial forces were disregarded. Furthermore, considering the confinement effects and its changes as a result of changing the axial forces of beam-column elements is relatively rare. In addition, comparing the responses of updated and traditional pushover analyses, it is illustrated how much considering the progressive changes of the moment-curvature characteristics throughout pushover analysis can affect the responses.

This study focuses on a new pushover analysis to update the moment-curvature properties of beam-column elements based on the axial force of these members during the analysis. To do so, pushover analysis is conducted on three RC moment resisting frames with 3-, 7-, and 10-story. The base shear-roof displacement curves of these frames are achieved once with a moment-curvature curve for each beam-column element that remains constant throughout the analysis and again with updating the moment-curvature properties of the beam-columns during the analysis. It is worth emphasizing that the tri-linear moment-curvature relations are used for the calculation of the moment-curvature properties; therefore, the assumptions were made in these relations to best fit with test results are presented in the current study. Confining action is considered using the developed method by Mander et al. (1988). Using of the linear flexibility model developed by Kunnath and Reinhorn (1989) as a reputable macro plasticity model, the nonlinear behavior of beam-column elements is modeled. Moreover, the comparison of responses in this study is limited to three RC moment resisting frames, so future works are required to be done for expanding knowledge concerning different lateral load systems, different connection systems, and so on.

2. Nonlinear Analysis

2.1. Moment-Curvature Relation

Regarding the nonlinear behavior of RC sections, the tri-linear moment-curvature relation is used (Figure 1) (Reinhorn et al. 2009). Three distinctive portions consisting of elastic, cracked, and yield states are shown in Figure 1. The moment-curvature properties are affected by the elasticity modulus of concrete and steel, the modulus of the rupture, and the compressive strength of concrete, the yield strength of steel, the ultimate strain of concrete, the yield strain of steel, dimensions, and the moment of inertia of section, etc. The following relations are used to define the moment-curvature properties.

a) Cracking state:

$$M_{cr} = \frac{f_r I}{(h-y)} + \frac{Nd}{6} \quad (1)$$

$$\varphi_{cr} = \frac{f_r}{E_c(h-y)} \quad (2)$$

b) Yielding state:

$$M_y = 0.5 f_c b_t d^2 (h-c)^2 [(1+\beta - \eta) n_0 + (2-\eta)\rho + (\eta - 2\beta)\alpha\rho'] \quad (3)$$

$$\varphi_y = \frac{c\varepsilon_y}{(1-k)d} \quad (4)$$

c) Ultimate state:

$$M_u = (1.24 - 0.15p - 0.5n_0) M_y \quad (5)$$

$$\frac{\varphi_u}{\varphi_y} = \frac{\beta_1 \varepsilon_u E_s}{f_y} \frac{(1-k)}{\left(R^2 + S\frac{c}{d}\right) - \frac{R}{(h-c)}} \quad (6)$$

where

$$R = \frac{(\rho' \varepsilon_u E_s - \rho f_y)(h-c)}{(1.7 f_c)} \quad (7)$$

$$S = \frac{\rho' \varepsilon_u E_s \beta_1 c (h-c)}{(0.85 f_c)} \quad (8)$$

Full details dealing with other parameters were presented in Habibi (2011).

The flexural stiffness of elastic, cracked,

and yield branches (Figure 1) can be calculated for the ends of the member as follows.

$$EI_{p1} = \frac{M_{crp}}{\varphi_{crp}} \qquad M \le M_{cr} \tag{9}$$

$$EI_{p2} = \frac{M_{yp} - M_{crp}}{\varphi_{yp} - \varphi_{crp}} \qquad M_{cr} < M \le M_y \tag{10}$$

$$EI_{p3} = \frac{M_{up} - M_{yp}}{\varphi_{up} - \varphi_{yp}} \qquad M_y < M \le M_u \tag{11}$$

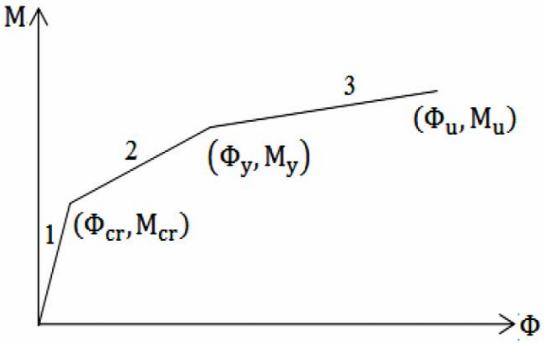

Fig. 1. Tri-linear moment curvature curve

The vertex-oriented hysteric model (Reinhorn et al., 2009) is applied in this study. Lateral pressure significantly affects the stress-strain relationship of compressed concrete. In contrast with unconfined concrete, confining concrete provides a higher resistance to internal cracking, ultimate strain, and axial strength. The concrete core of columns should be confined to retain flexural strength as high curvatures in the plastic hinges. In other words, to achieve ductile performance, the higher axial compressive load requires a higher amount of confining reinforcement (Mander et al., 1988). The confinement of concrete boosts the strength coupled with the ductility of compressed concrete.

The enhanced strength along with the slope of the descending branch of the concrete stress-strain curve improves the flexural strength and ductility of RC columns. When the compressive strength reaches, in contrast to the core concrete keeping bearing stress at a high level of strains, the cover concrete will not be efficient because of an unconfined situation. Confining the compressed concrete, preventing the buckling of the longitudinal bars and a shear failure are some advantages of the transverse reinforcements. In the current study, the stress-strain model of Mander et al. (1988) is applied to take the confining action into consideration (Figure 2).

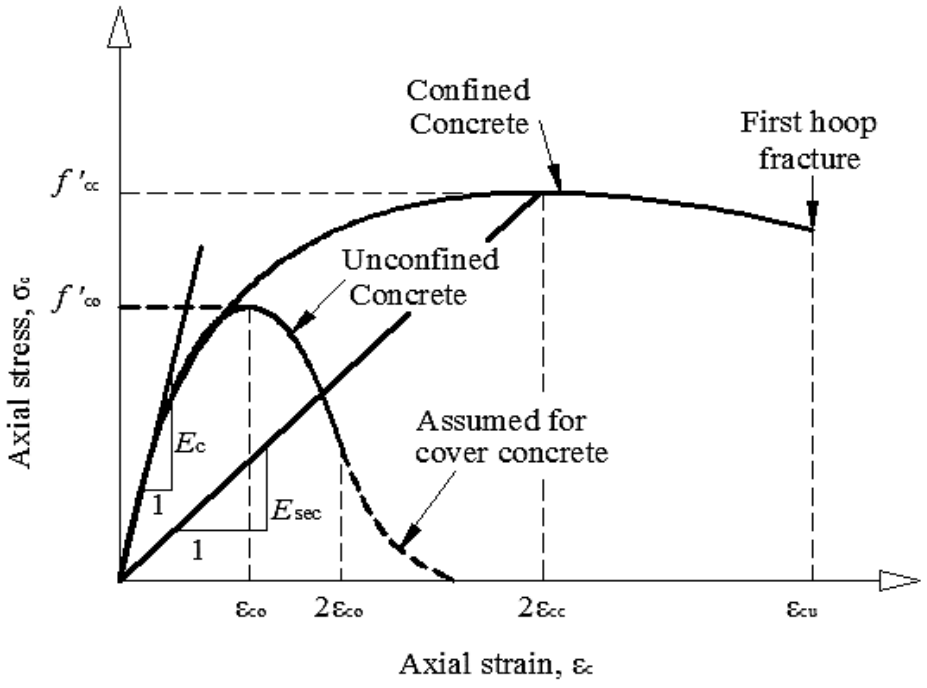

Fig. 2. Stress-strain model (Mander et al., 1988)

2.2. Stiffness Matrix

The linear plasticity model developed in Kunnath and Reinhorn (1989) is used to simulate the nonlinear behavior of beam-column members. The macro plasticity models are categorized into two classes, a) lumped and b) distributed plasticity models. In the lumped plasticity models, the plasticity is concentrated in the two ends of beam-column elements. The member between these ends stays elastic. In RC members, inelastic deformations are spread throughout the member, hence the concentrated plasticity models do not comply with the inelastic behavior of these elements. In spread plasticity models, a predefined distribution for flexural flexibility along the elements' length is assumed. In the linear plasticity model (Figure 3), the inelastic zones encounter variations in flexibility and the rest of the member stays elastic.

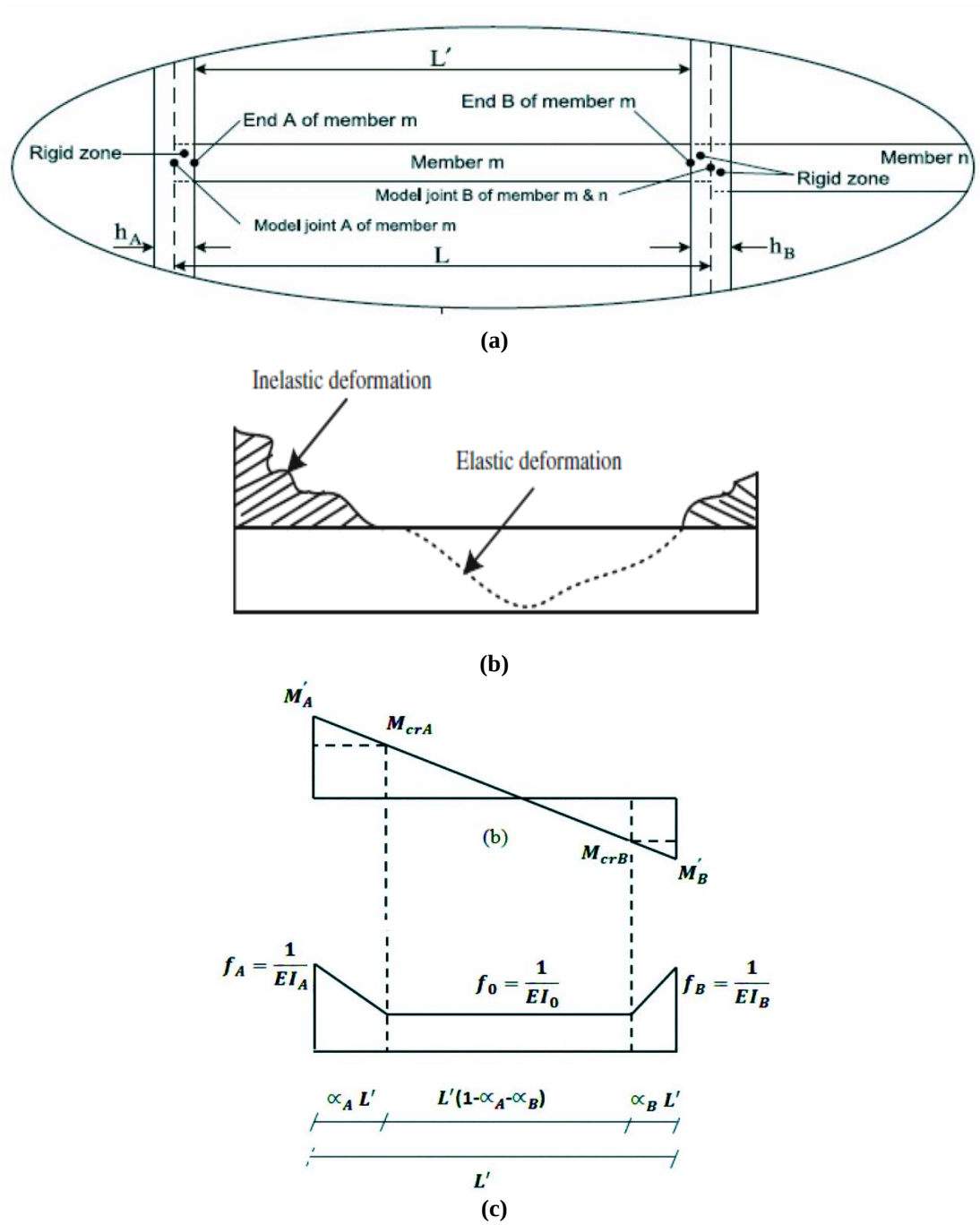

Fig. 3. a) Rigid zone and ends definitions of a RC element; b) Moment distribution; and C) Linear flexibility distribution (Reinhorn et al., 2009)

The cracked parts of the element at the ends are defined via the yield penetration coefficients ($\propto_A$ and $\propto_B$) (Reinhorn et al., 2009). The element stiffness matrix relating the rotations and moments at the member ends is defined as follows.

$$\begin{bmatrix} M'_A \\ M'_B \end{bmatrix} = \begin{bmatrix} K_{AA} & K_{AB} \\ K_{BA} & K_{BB} \end{bmatrix} \begin{bmatrix} \theta'_A \\ \theta'_B \end{bmatrix} = [\mathrm{K}`] \begin{bmatrix} \theta'_A \\ \theta'_B \end{bmatrix} \quad (12)$$

The components of the stiffness matrix are calculated as follows.

$$K_{AA} = \frac{12EI_0EI_AEI_B}{L'D_{et}} \left(L'^2 GA_z f'_{BB} + 12EI_0EI_AEI_B\right) \quad (13)$$

$$K_{BB} = \frac{12EI_0EI_AEI_B}{L'D_{et}} \left(L'^2 GA_z f'_{AA} + 12EI_0EI_AEI_B\right) \quad (14)$$

$$K_{AB} = K_{BA} = \frac{-12EI_0EI_AEI_B}{L'D_{et}} \left(L'^2 GA_z f'_{AB} + 12EI_0EI_AEI_B\right) \quad (15)$$

$$D_{et} = L'^2 GA_z \left(f'_{AA} f'_{BB} - f'^2_{AB}\right) + 12EI_0EI_AEI_B \left(f'_{AA} + f'_{BB} - 2f'_{AB}\right) \quad (16)$$

$$f'_{AA} = 4EI_AEI_B + 4EI_B(EI_0 - EI_A)(3 \propto_A - 3 \propto_A^2 + \propto_A^3) + 4EI_A(EI_0 - EI_B) \propto_B^3 \quad (17)$$

$$f'_{AB} = 2EI_AEI_B + EI_B(EI_0 - EI_A)(2 \propto_A^2 - \propto_A^3) + EI_A(EI_0 - EI_B)(2 \propto_B^2 - \propto_B^3) \quad (18)$$

$$f'_{BB} = 4EI_AEI_B + EI_B(EI_0 - EI_A)(\propto_A^3) + EI_A(EI_0 - EI_B)(6 \propto_B - 4 \propto_B^2 + \propto_B^3) \quad (19)$$

where GA_0: is the shear stiffness of an element. To consider the rigid zone effects and shear components are calculated as Habibi (2011).

Bending moments and axial forces are presumed uncoupled.

$$\begin{bmatrix} Y_a \\ Y_b \end{bmatrix} = \frac{EA}{L} \begin{bmatrix} 1 & -1 \\ -1 & 1 \end{bmatrix} \begin{bmatrix} v_a \\ v_b \end{bmatrix} = [\mathrm{K_a}] \begin{bmatrix} v_a \\ v_b \end{bmatrix} \quad (20)$$

Assembling the above-mentioned stiffness matrices, the tangential stiffness matrix is obtained.

To consider $P-\Delta$ effect, a geometric stiffness matrix is added to the tangential stiffness matrix (Eq. (21)).

$$\mathrm{K_g} = {}^{N}/_{L} \begin{bmatrix} 0 & & & & & \\ 0 & 6/5 & & \text{symmetric} & & \\ 0 & L/10 & 2L^2/15 & & & \\ 0 & 0 & 0 & 0 & & \\ 0 & -6/5 & -L/10 & 0 & 6/5 & \\ 0 & L/10 & -L^2/30 & 0 & -L/10 & 2L^2/15 \end{bmatrix} \quad (21)$$

The geometric matrix depends on the axial load and the length of the element (N and L). The modified Newton-Raphson procedure is used for nonlinear analysis and to achieve the internal forces.

2.3. Pushover Analysis

A structure can behave between entirely elastic and collapse states. A nonlinear analysis is necessary to expand knowledge about the actual demands of structures (especially those subjected to severe ground motions). Pushover analysis is a nonlinear procedure that is widely used as the main tool for the inelastic analysis of structures. In pushover analysis, firstly, the gravity loads are exerted on the building frame. After that, the lateral loads are monotonically increased while the structure gravity loads remain constant. The lateral loads are distributed along the height of the structure based on a predefined pattern. In this study, the lateral load pattern recommended by FEMA273 is used.

$$\Delta F_i = \frac{W_i h_i^k}{\sum_{i=0}^{N} W_i h_i^k} \Delta V_b$$

$$k = \begin{cases} 1 & T < 0.5 \\ 0.5T + 0.75 & 0.5 \le T \le 2.5 \\ 2 & T > 2.5 \end{cases} \quad (22)$$

3. Numerical Study

The applicability and the efficiency of the developed procedure are assessed through three numerical case studies. The roof displacement-base shear curves of these frames are calculated once with a constant moment-curvature remaining constant throughout the analysis and again regarding the progressive changes of the moment-

curvature relations based on the axial forces updated during the analysis (henceforth named convenient and updated pushover analysis, respectively).

3.1. Case Study 1

The first example is an asymmetric 3-story, 3-bay moment-resisting reinforced concrete frame (Izadpanah and Habibi, 2018a) (Figure 4) in which the width and height of all beams and columns are 300 mm. All beams possess the reinforcement of 763 mm^2 at the bottom and top. The reinforcement of all columns on each face is 763 mm^2. The concrete has a cylinder strength of 20 MPa. The concrete presents a strain of 0.002 regarding the maximum strength. The ultimate strain of concrete is 0.003. The concrete has a modulus of rupture of 2.82 MPa and a modulus of elasticity of 22360 MPa. The yield strength and modulus of elasticity of steel are 300 MPa and 200000 MPa, respectively. A uniformly-distributed gravity load exerted on the beams of each story is 20 kN/m. A cover to the reinforcement centroid of 50 mm is assumed.

The convenient and updated pushover analysis of this frame is conducted inclusion/exclusion of the confinement effect (CE). The roof displacement-base shear curves are compared in Figure 5. In Figure 6, the roof displacement-base shear curves of this frame from Izadpanah and Habibi (2018a) are depicted.

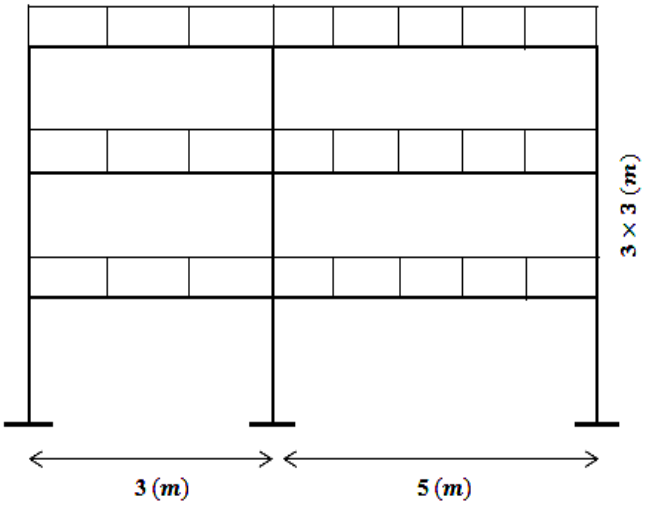

Fig. 4. Tri-linear moment curvature curve

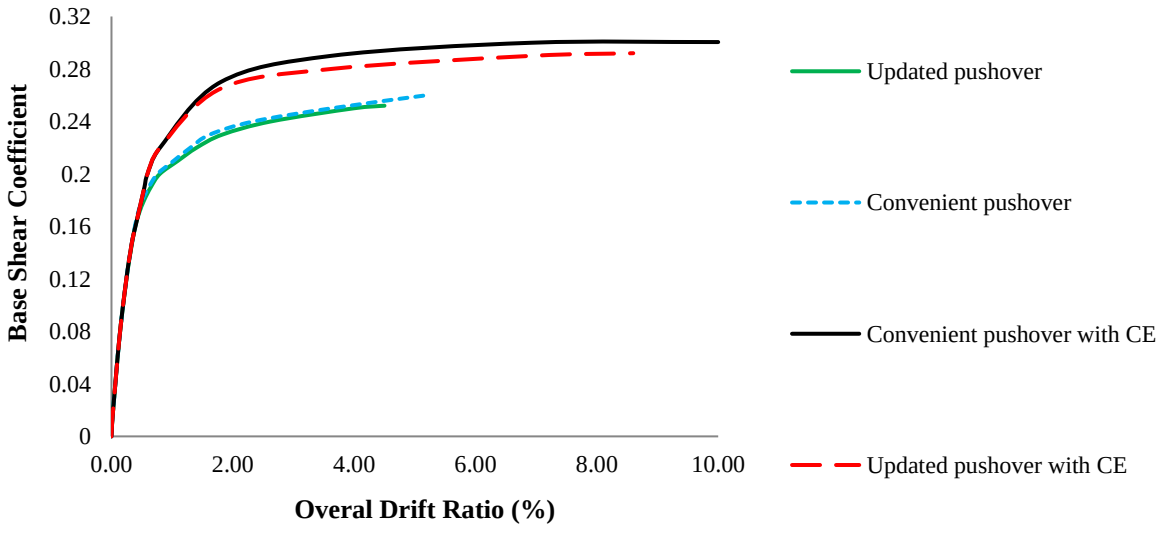

Fig. 5. The roof displacement-base shear curves of 3-story frame

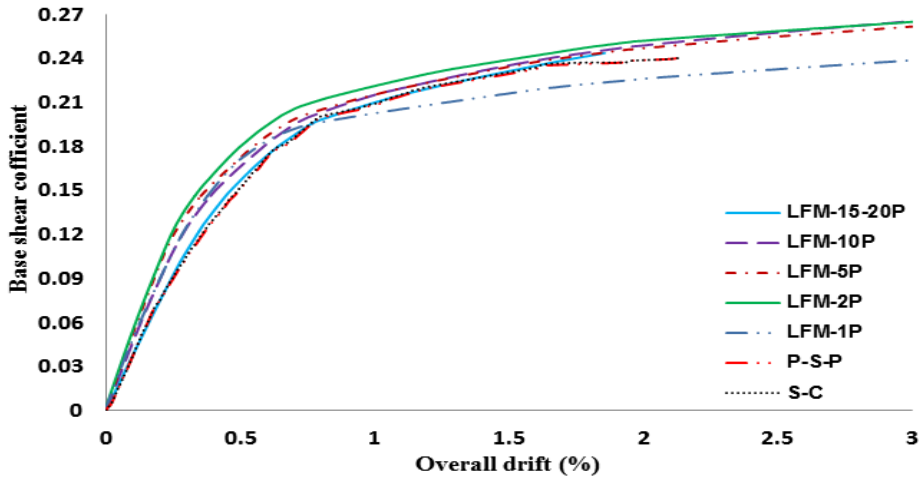

Fig. 6. The roof displacement-base shear curves of 3-story frame (Izadpanah and Habibi, 2018a)

As shown in Figure 5, considering the confinement effect leads to an enhancement in the lateral load-resisting characteristics of the frame. In comparison with the unconfined state, the secant stiffness, energy dissipation capacity, ductility, and ultimate strength of the confined frame are boosted. For convenient pushover analysis, the ductility and ultimate base shear coefficient of the confined frame are around 9 and 0.3 whereas those of the unconfined frame are 6.5 and 0.26. For the updated pushover analysis, the values of the ductility, and ultimate base shear coefficient of the confined frame are 7.75 and 0.29, and those of the unconfined frame are 5.6 and 0.25. The second stiffness of the confined frame is around 1.2 times of the unconfined frame in the overall drift ratio of 2% and 4%.

Comparing the curves of updated and convenient pushover analyses indicates that updating moment-curvature properties of the beam-column elements results in decreasing the ductility of the frame. For the confined frame, the ultimate strength of a convenient pushover is higher than the updated one. On the contrary, for the unconfined frame, the difference is negligible. Comparing the convenient pushover curve in Figure 5 and LFM-1P curve in Figure 6 confirms the accuracy of the procedure applied in this study.

3.2. Case Study 2

A 7-story, 3-bay planner reinforced concrete frame as the second example is evaluated (Figure 7) (Izadpanah and Habibi, 2018b). The cross-section properties of this frame are listed in Table 1. Concrete has a cylinder strength of 38 Mpa and a strain of 0.002 regarding the maximum strength. The ultimate strain of concrete is assumed as 0.006. Steel possesses the yield strength and modulus of elasticity of 300 MPa and 200000 MPa, respectively. On all beams, a uniform gravity load of 30 kN/m is exerted. Each story has a height of 3.2 m and the length of each bay is 5 m.

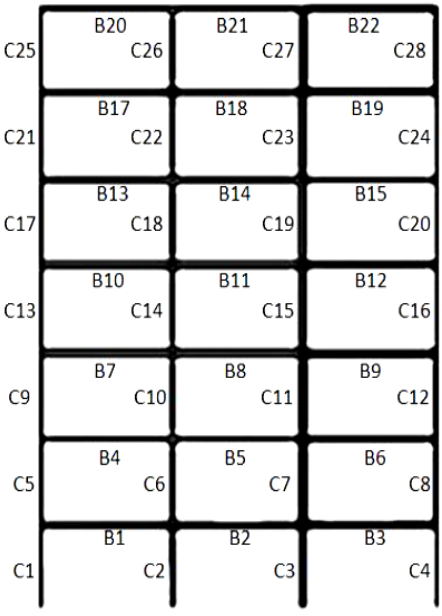

Fig. 7. Geometry of seven-story RC frame

The convenient and updated pushover analyses of this frame are performed and the roof displacement-base shear curves are compared in Figure 8.

Table 1. The cross section properties of seven-story RC frame

Element type	Dimension (mm)		Reinforcement	
Beam	Width	Height	Bottom	Top
1st to 5th story	300	450	3Ø20	7Ø20
6th and 7th story	350	400	3Ø20	4Ø20
Column	Dimension (mm)		Reinforcement on each face	
	Width	Height		
1st story	500	500	7Ø20	
2nd and 3rd story	500	500	6Ø20	
4th and 5th story	450	450	5Ø20	
6th and 7th story	350	350	5Ø20	

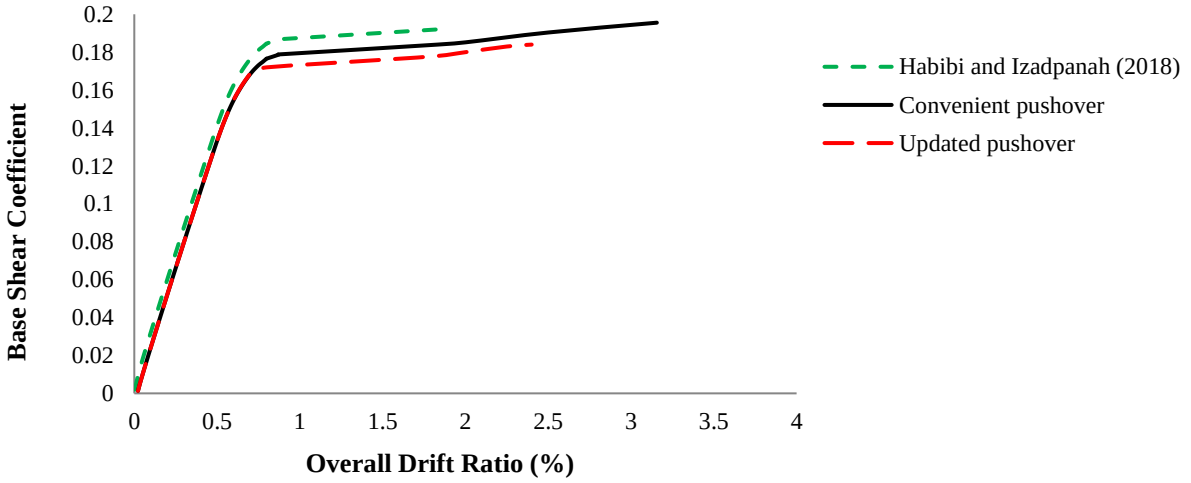

Fig. 8. The roof displacement-base shear curves of 7-story frame

As shown in Figure 8, for updated pushover procedure, the lateral load-carrying capacity of the frame is weakened in comparison with the convenient pushover method. In other words, considering the progressive changes of moment-curvature properties of columns leads to reducing the ductility coupled with the ultimate strength of the frame (around 30% and 6%). The convenient pushover curve complies with that of Izadpanah and Habibi (2018b). The gap between the convenient pushover curve and Izadpanah and Habibi (2018b) is due to the different plasticity models considered in these studies. Izadpanah and Habibi (2018b) used an improved linear plasticity model to consider the gravity load effects. They proved that when a member is subdivided into several elements, the responses of the linear plasticity model converge to the improved linear plasticity model that used one element for each member. In Figure 9, the changes in axial force of columns C_1, C_2, C_9, C_{10}, C_{17}, C_{18}, C_{25}, and C_{26} throughout the pushover analysis are indicated. In Figure 10, the moment-curvature curves of column C_1 at the first and the last steps of pushover analysis are demonstrated.

As indicated in Figure 9, the axial force of edge columns significantly varies throughout the pushover analysis and these changes for lower story columns are higher e.g. the axial load of C_1 reaches 9.88 kN in overall drift of 2.4% from 54 kN in the first step of analysis that means around 80 percent reduction. The axial load changes reduce for higher story columns e.g. the axial load of C_{25} reduces to 4 kN in overall drift 2.4% from 7 kN in the first step of analysis which means around 40 percent reduction. For middle columns, the variation of axial forces is negligible. Comparing the moment-curvature curves of C_1 in Figure 10 shows how axial load can affect the moment-curvature properties of columns. As it is clear, the flexural properties of C_1 including cracking, yielding, ultimate moments, and also

stiffness of all branches decrease along the analysis. Since during the pushover analysis on one side of frames, the axial forces of edge columns decrease and on another side, the axial forces increase; therefore, the gap between capacity curves of convenient and updated pushover analysis is not significant. However, the changes in moment-curvature properties of columns especially edge columns in the lower levels affect the behavior and demands of columns.

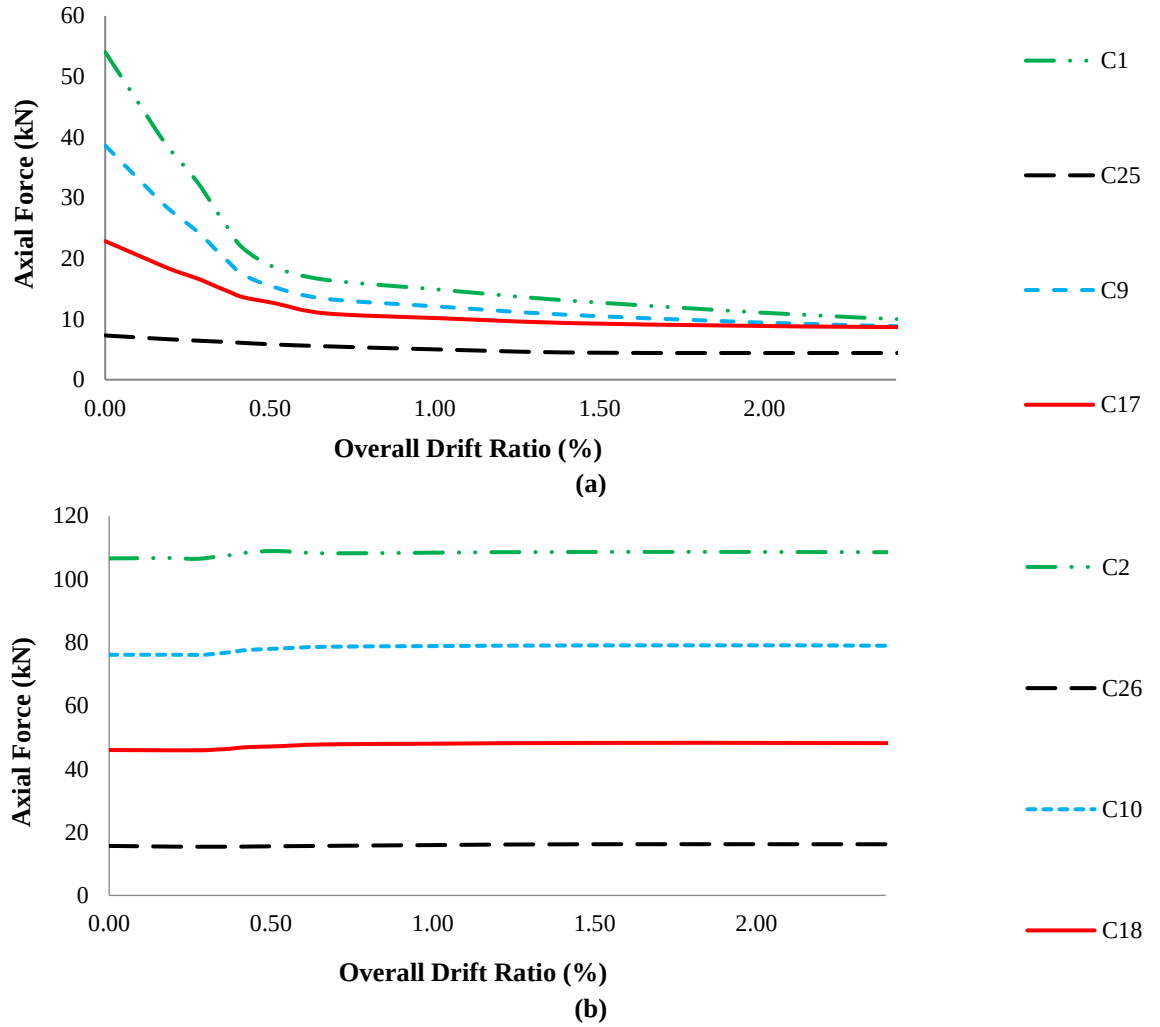

Fig. 9. The changes in axial forces of the columns: a) Edge columns; and b) Middle columns

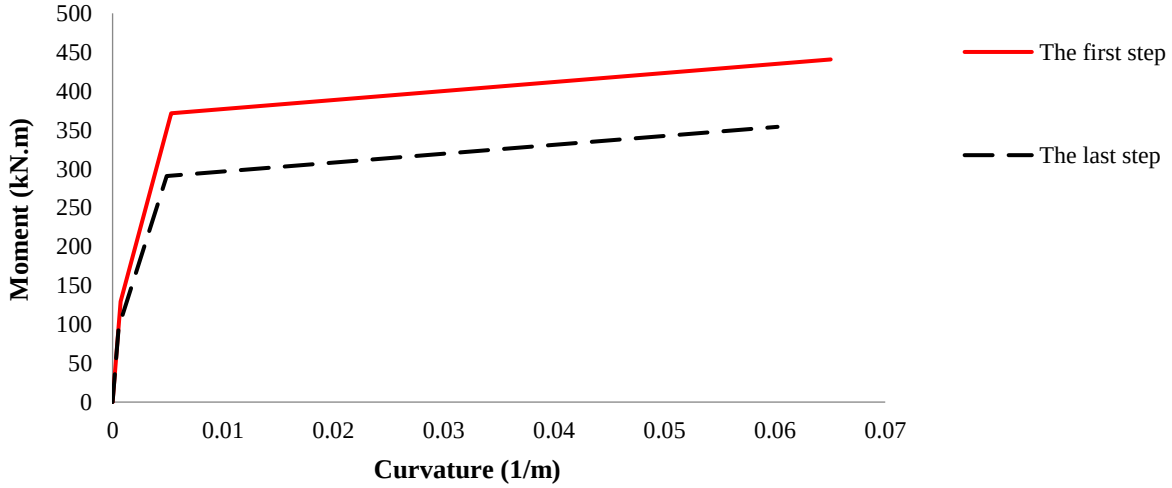

Fig. 10. The moment-curvature curve of column C_1 at the first and the last steps of pushover analysis

3.3. Case Study 3

The third example is a 10-story, 2-bay planner reinforced concrete moment-resistant frame indicated in Figure 11 (Izadpanah and Habibi, 2018a). A cylinder strength of 30 MPa and a modulus of rupture of 3.45 MPa are assumed for concrete. Concrete has a modulus of elasticity of 27,400 MPa and an ultimate strain of 0.004. A strain of 0.002 regarding the maximum strength is considered for concrete. The steel is assumed to possess a yield strength of 300 MPa and a modulus of elasticity of 200,000 MPa. The distributed gravity load of 35 KN/m is assumed to impose on the beams. In Figure 12, the roof displacement-base shear curves of the convenient- and updated pushover analysis of this frame are shown.

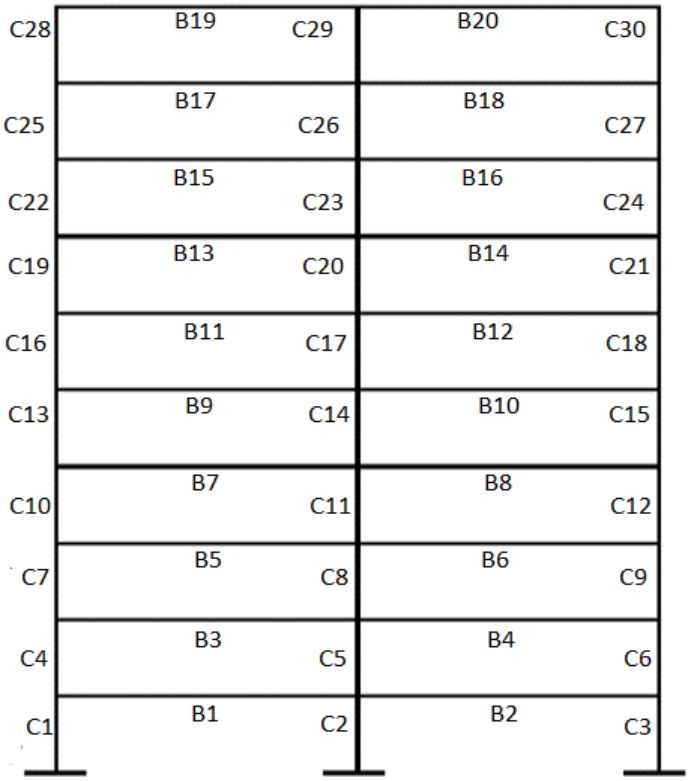

Fig. 11. Ten-story RC frame

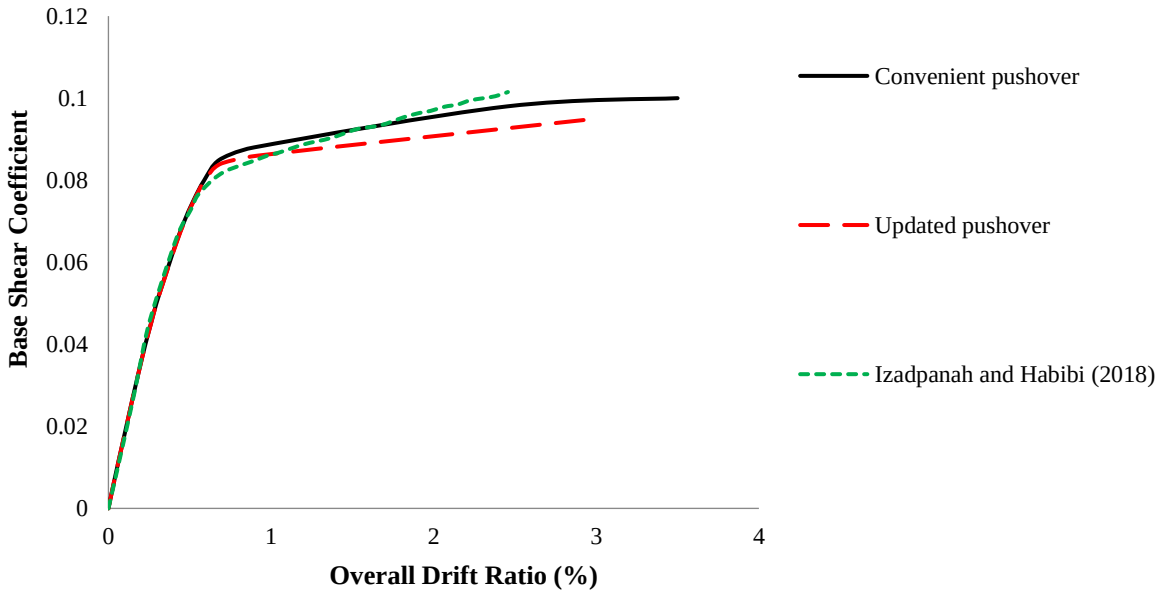

Fig. 12. The roof displacement-base shear curves of 10-story frame

As shown in Figure 12, the roof displacement-base shear curve acquired in this study is in good agreement with that of Izadpanah and Habibi (2018a). Considering the influence of the changes of the axial load on the moment-curvature of beam-column elements results in a reduction in the lateral load resistance of the frame. The secant stiffness, energy dissipation capacity, ductility, and ultimate strength of the updated pushover are lower than the convenient one. In Figure 13, the variation of axial force of column C_1 during the pushover analysis and the moment-curvature curve of this column at the first and the last steps of pushover analysis calculated using Opensees (fiber-based analysis) are demonstrated.

As indicated in Figure 13, the axial force of edge columns at the last step of the pushover analysis is around 3% of that of the first step of the analysis. The yielding and ultimate moments at the last step are significantly lower than the first step of the analysis. On the contrary, the ductility of the column in the last step is higher than in the first step.

4. Conclusions

The moment-curvature properties of the beam-column elements depend on the axial load of these elements. The pushover analysis as a way capable of providing valuable information about the behavior of structures from elastic to collapse has become a popular procedure of engineers. In the pushover analysis, in common, the moment-curvature properties of beam-column elements are achieved based on the axial forces achieved at the first step of analysis (regarding the gravity loads) and remain constant throughout the analysis. This study focused on developing a new pushover analysis to account for updating the moment-curvature properties of beam-column elements during the analysis. The updated pushover analysis was applied on three reinforced concrete frames and the roof displacement-base shear curves were compared with those of convenient pushover analysis. As per the outcomes, the following can be summarized.

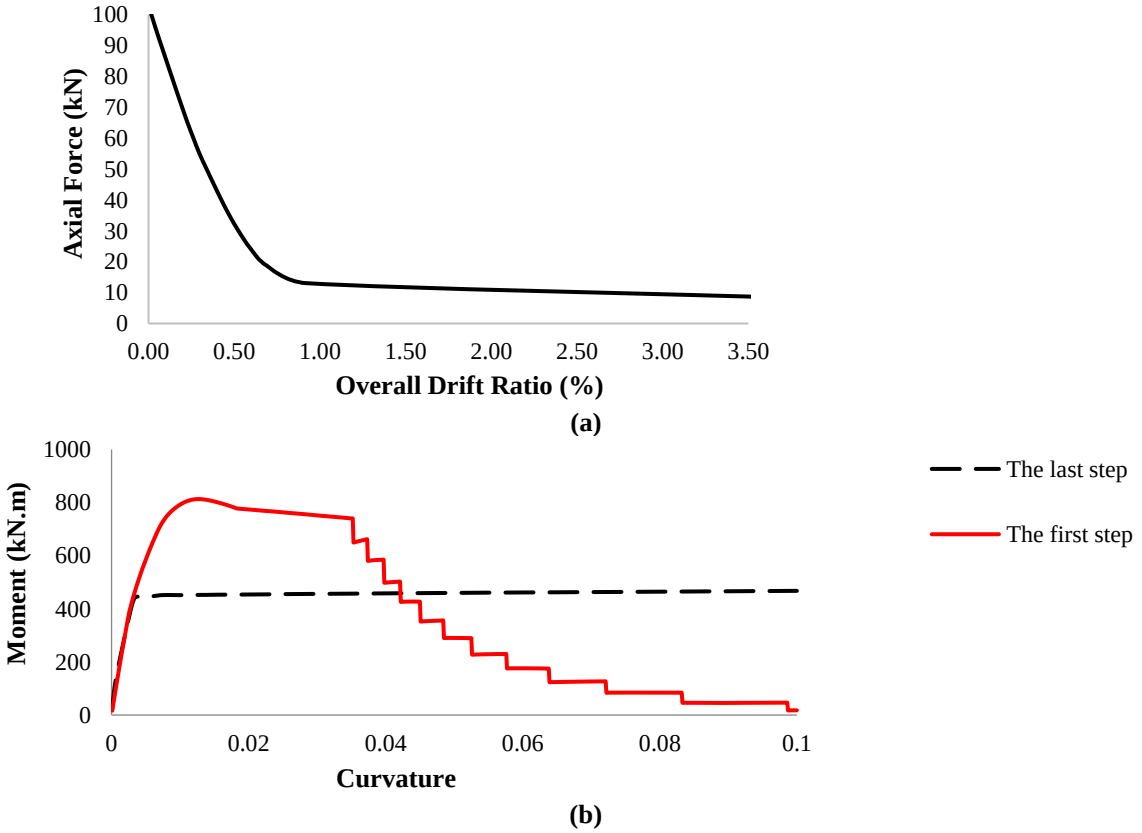

Fig. 13. The beam-column C_1: a) The changes of axial forces; and b) The moment-curvature curves

- Updating the moment-curvature properties leads to reducing the lateral load-carrying capacity of the frames e.g. ductility, ultimate strength, second stiffness, and so on. This reduction for higher frames is more significant than for lower ones.
- In comparison with the unconfined condition, when the confinement effect is considered, the gap between updated- and convenient-pushover analysis increases.
- The changes in axial loads during the pushover analysis for the edge columns located in the lower stories are higher than those placed in higher levels or middle columns. Therefore, the moment-curvature properties of the edge columns in the lower stories e.g., cracking, yielding, and ultimate moments are higher than others.
- The moment-curvature properties of beam-column elements significantly depend on the axial forces. In pushover analysis, the axial force of one side of the frame increases and another side decreases; therefore, the gap between the roof displacement-base shear curves of updated- and convenient-pushover analysis is not significant. Despite the low differences between the roof displacement-base shear curves of updated- and convenient-pushover analysis, the changes in axial force of beam-column members can significantly affect the responses of these members.

Further research could determine the influence of changing the moment-curvature properties of beam-column elements and confining action on the responses of reinforced concrete frames with various geometry and material properties, different lateral load systems, different connection systems, and so on.

5. Symbols

E_c	Modulus of elasticity of concrete	M_{crB}	Cracking moment at the end ‘B’
E_s	Modulus of elasticity of concrete	$\propto_A$	Cracked part at the end ‘A’
f_r	Concrete modulus of rupture	$\propto_B$	Cracked part at the end ‘B’
f_c	Cylinder strength of concrete	M'_A	Moment at the member’ end ‘A’
f_y	Yield strength of steel	M'_B	Moment at the member’ end ‘B’
ε_y	Yield strain of steel	θ'_A	Rotation at the member’ end ‘A’
ε_u	Ultimate strain of concrete	θ'_B	Rotation at the member’ end ‘B’
β_1	Depends on the strength of concrete	GA_0	Shear stiffness
N	Axial force	Y_a	Axial force
h	Height of section	Y_b	Axial force
c	Cover-to-steel centroid	v_a	Axial displacement
b_t	Top width of section	v_b	Axial displacement
y	Distance from the section neutral axis to the extreme fiber in tension	$\frac{EA}{L}$	Axial stiffness of element
I	Moment of inertia of the section	L	Length of the element
$1/EI_A$	Sections’ flexural flexibility regarding the end ‘A’	h_i	Distance from base to i^{th} story level
$1/EI_B$	Sections’ flexural flexibility regarding the end ‘B’	W_i	Seismic weight at i^{th} story level
$1/EI_0$	Flexibility in the elastic part of the member	T	Main vibration period of the building
M_{crA}	Cracking moment at the end ‘A’		

6. References

Amini, M.A. and Poursha, M. (2018). "Adaptive force-based multimode pushover analysis for seismic evaluation of midrise buildings", *Journal of Structural Engineering*, 144(8), 04018093, https://doi.org/10.1061/(ASCE)ST.1943-541X.0002070.

Antoniou, S. and Pinho, R. (2004). "Development and verification of a displacement-based adaptive pushover procedure", *Journal of earthquake engineering*, 8(05), 643-661, https://doi.org/10.1142/S136324690400150X.

ATC-40, (1997), "Seismic evaluation and retrofit of concrete buildings", Applied Technology Council, California Seismic Safety Commission.

Bakalis, A.P. and Makarios, T.K. (2021). "Seismic enforced-displacement pushover procedure on multistorey R/C buildings", *Engineering Structures*, 229, 111631, https://doi.org/10.1016/j.engstruct.2020.111631.

Cao, X.Y., Feng, D.C. and Wu, G. (2021). "Pushover-based probabilistic seismic capacity assessment of RCFs retrofitted with PBSPC BRBF sub-structures", *Engineering Structures*, 234, 111919, https://doi.org/10.1016/j.engstruct.2021.111919.

CEN. (2004), "Eurocode 8: Design of structures for earthquake resistance. Part 1: General rules, seismic actions and rules for buildings", EN 1998-1, CEN, Brussels, December.

Chopra, A.K. and Goel, R.K. (2002). "A modal pushover analysis procedure for estimating seismic demands for buildings", *Earthquake Engineering & Structural dynamics*, 31(3), 561-582, https://doi.org/10.1002/eqe.144.

Chopra, A.K. and Goel, R.K. (2004). "A modal pushover analysis procedure to estimate seismic demands for unsymmetric-plan buildings", *Earthquake Engineering & Structural Dynamics*, 33(8), 903-927, https://doi.org/10.1002/eqe.380.

Costa, R., Providencia, P. and Ferreira, M. (2017). "Influence of joint modelling on the pushover analysis of a RC frame", *Structural Engineering and Mechanics: An International Journal*, 64(5), 641-652, https://doi.org/10.12989/sem.2017.64.5.641.

Daei, A. and Poursha, M. (2021). "On the accuracy of enhanced pushover procedures for seismic performance evaluation of code-conforming RC moment-resisting frame buildings subjected to pulse-like and non-pulse-like excitations", *Structures*, 32, 929-945, https://doi.org/10.1016/j.istruc.2021.03.035.

Dehghani, E. and Soltani Mohajer, M. (2022). "Development of the fragility curves for conventional reinforced concrete moment resistant frame structures in Qods Town, Qom City, Iran", *Civil Engineering Infrastructures Journal*, 55(1), 31-41, https://doi.org/10.22059/CEIJ.2021.306156.1690.

Elnashai, A.S. (2001). "Advanced inelastic static (pushover) analysis for earthquake applications", *Structural Engineering and Mechanics*, 12(1), 51-70, https://doi.org/10.12989/sem.2022.84.1.085.

Fajfar, P. and Fischinger, M. (1988). "N2-A method for non-linear seismic analysis of regular buildings", In: *Proceedings of the Ninth World Conference in Earthquake Engineering*, (Vol. 5, pp. 111-116).

Fajfar, P. and Gašperšič, P. (1996). "The N2 method for the seismic damage analysis of RC buildings", *Earthquake Engineering & Structural Dynamics*, 25(1), 31-46, https://doi.org/10.1002/(SICI)1096-9845(199601)25:1<31::AID-EQE534>3.0.CO;2-V.

Faruk, M.O., Singh, S.K. and Mondal, S. (2023). "Comparative study of buckling restrained braces and fluid viscous damper applied in an RCC structure following pushover analysis", *Materials Today: Proceedings*, https://doi.org/10.1016/j.matpr.2023.03.471.

FEMA273, (1997), "NEHRP guideline for the seismic rehabilitation of buildings", Federal Emergency Management Agency, Washington, DC.

Ghayoumian, G. and Emami, A.R. (2020). "A multi-direction pushover procedure for seismic response assessment of low-to-medium-rise modern reinforced concrete buildings with special dual system having torsional irregularity", *Structures*, 28, 1077-1107, https://doi.org/10.1016/j.istruc.2020.09.031.

Gulkan, P. and Sozen, M.A. (1974). "Inelastic responses of reinforced concrete structure to earthquake motions", *Journal Proceedings*, 71(12), 604-610.

Gupta, A. and Krawinkler, H. (2000). "Estimation of seismic drift demands for frame structures", *Earthquake Engineering & Structural Dynamics*, 29(9), 1287-1305, https://doi.org/10.1002/1096-9845(200009)29:9%3C1287::AID-EQE971%3E3.0.CO;2-B.

Habibi, A.R. (2011). "Nonlinear sensitivity of analysis of RCMRF considering both axial and felexure effects", *IJE Transactions A: Basics*, 24(3), 223-238, https://doi.org/10.5829/idosi.ije.2011.24.03a.02.

Habibi, A., Saffari, H. and Izadpanah, M. (2019). "Optimal lateral load pattern for pushover

analysis of building structures", *Steel and Composite Structures*, 32(1), 67-77, https://doi.org/10.12989/scs.2019.32.1.067.

Hassan, W.M. and Reyes, J.C. (2020). "Assessment of modal pushover analysis for mid-rise concrete buildings with and without viscous dampers", *Journal of Building Engineering*, 29, 101103, https://doi.org/10.1016/j.jobe.2019.101103.

Izadpanah, M. and Habibi, A. (2018b). "Evaluating the accuracy of a new nonlinear reinforced concrete beam-column element comprising joint flexibility", *Earthquakes and Structures*, 14(6), 525-535, https://doi.org/10.12989/eas.2018.14.6.525.

Izadpanah, M. and Habibi, A. R. (2018a). "New spread plasticity model for reinforced concrete structural elements accounting for both gravity and lateral load effects", *Journal of Structural Engineering*, 144(5), 04018028, https://doi.org/10.1061/(ASCE)ST.1943-541X.0002016.

Jalilkhani, M., Ghasemi, S.H. and Danesh, M. (2020). "A multi-mode adaptive pushover analysis procedure for estimating the seismic demands of RC moment-resisting frames", *Engineering Structures*, 213, 110528, https://doi.org/10.1016/j.engstruct.2020.110528.

Kalkan, E. and Kunnath, S.K. (2006). "Adaptive modal combination procedure for nonlinear static analysis of building structures", *Journal of Structural Engineering*, 132(11), 1721-1731, https://doi.org/10.1016/j.engstruct.2020.110528.

Kheirollahi, M., Abedi, K. and Chenaghlou, M.R. (2021). "A new pushover procedure for estimating seismic demand of double-layer barrel vault roof with vertical double-layer walls", *Structures*, 34, 1507-1524, https://doi.org/10.1016/j.istruc.2021.08.090.

Krawinkler, H. and Seneviratna, G.D.P.K. (1998). "Pros and cons of a pushover analysis of seismic performance evaluation", *Engineering Structures*, 20(4-6), 452-464, https://doi.org/10.1016/S0141-0296(97)00092-8.

Kunnath, S.K. and Reinhorn, A.M. (1989). "Inelastic three-dimensional response analysis of reinforced concrete building structures (IDARC-3D)", National Center for Earthquake Engineering Research, Buffalo, NY.

Lawson, R.S., Vance, V. and Krawinkler, H. (1994). "Nonlinear static pushover analysis, why, when and how", In: *Proceedings of Fifth US National Conference on Earthquake Engineering*, (Vol. 1, p. 283), Chicago, IL.

Lherminier, O., Erlicher, S., Huguet, M. and Barakat, M. (2023). "The E-DVA method for multi-modal pushover analysis and dominant modes", *Procedia Structural Integrity*, 44, 528-535, https://doi.org/10.1016/j.prostr.2023.01.069.

Lu, X. and Li, J. (2023). "The evaluation of the seismic performance of tall bridge piers with non-adaptive pushover methods", *Structures*, 48, 839-851, https://doi.org/10.1016/j.istruc.2023.01.021.

Mander, J.B., Priestley, M.J. and Park, R., (1988). "Theoretical stress-strain model for confined concrete", *Journal of Structural Engineering*, 114(8), 1804-1826, https://doi.org/10.1061/(ASCE)0733-9445(1988)114:8(1804).

Moradi, M. and Tavakoli, H. (2020). "Proposal of an energy based assessment of robustness index of steel moment frames under the seismic progressive collapse", *Civil Engineering Infrastructures Journal*, 53(2), 277-293, https://doi.org/10.22059/CEIJ.2019.283574.1591.

Mwafy, A.M. and Elnashai, A.S. (2001). "Static pushover versus dynamic collapse analysis of RC buildings", *Engineering Structures*, 23(5), 407-424, https://doi.org/10.1016/S0141-0296(00)00068-7.

Nazri, F.M. and Alexander, N.A. (2014). "Exploring the relationship between earthquake intensity and building damage using single and multi-degree of freedom models", *Canadian Journal of Civil Engineering*, 41(4), 343-356, https://doi.org/1139/cjce-2012-0477.

Nazri, F.M. and Alexander, N.A. (2015). "Predicting collapse loads for buildings subjected to seismic shock", *Bulletin of Earthquake Engineering*, 13(7), 2073-2093, https://doi.org/10.1007/s10518-014-9707-9.

Olivito, R.S. and Porzio, S. (2019). "A new multi-control-point pushover methodology for the seismic assessment of historic masonry buildings", *Journal of Building Engineering*, 26, 100926, https://doi.org/10.1016/j.jobe.2019.100926.

Ozgenoglu, M. and Arıcı, Y. (2017). "Comparison of ASCE/SEI Standard and modal pushover-based ground motion scaling procedures for pre-tensioned concrete bridges", *Structure and Infrastructure Engineering*, 13(12), 1609-1623, https://doi.org/10.1080/15732479.2017.1310258.

Rahmani, A.Y., Bourahla, N., Bento, R. and Badaoui, M. (2018). "An improved upper-bound pushover procedure for seismic assessment of high-rise moment resisting steel frames", *Bulletin of Earthquake Engineering*, 16(1), 315-339, https://doi.org/10.1007/s10518-017-0204-9.

Reinhorn, A.M., Roh, H., Sivaselvan, M.V., Kunnath, S.K., Valles, R.E., Madan, A., Li, C., Lobo, R. and Park, Y.J. (2009). "IDARC 2D

version 7.0: A program for the inelastic damage analysis of structures", MCEER Technical Report, MCEER-09-0006, State University of New York, Buffalo, NY.

Reyes, J.C. and Chopra, A.K. (2011). "Three-dimensional modal pushover analysis of buildings subjected to two components of ground motion, including its evaluation for tall buildings. *Earthquake Engineering and Structural Dynamics*, 40(7), 789-806, https://doi.org/10.1002/eqe.1060.

Tian, L. and Qiu, C. (2018). "Modal pushover analysis of self-centering concentrically braced frames", *Structural Engineering and Mechanics*: *An International Journal*, 65(3), 251-261, https://doi.org/10.12989/sem.2018.65.3.251.

Wang, J., Wang, X., Ye, A. and Guan, Z. (2023). "Deformation-based pushover analysis method for transverse seismic assessment of inverted Y-shaped pylons in kilometer-span cable-stayed bridges: Formulation and application to a case study", *Soil Dynamics and Earthquake Engineering*, 169, 107874, https://doi.org/10.1016/j.soildyn.2023.107874.

Worku, A.M. and Hsiao, P.C. (2022). "An improved first-mode-based pushover analytical procedure for assessing seismic performance of special moment resisting frame building structures", *Engineering Structures*, 252, 113587, 10.1016/j.engstruct.2021.113587.

Zhou, P., Xiong, Z., Chen, X. and Wang, J. (2023). "Seismic performance of RC frame structure across the earth fissure based on pushover analysis", *Structures*, 52, 1035-1050, https://doi.org/10.1016/j.istruc.2023.03.148.